Robust Coupling between Structural and Electronic Transitions in a Mott Material

Yoav Kalcheim,[1] Nikita Butakov,[2] Nicolas M. Vargas,[1] Min-Han Lee,[1,3] Javier del Valle,[1] Juan Trastoy,[1,*] Pavel Salev,[1] Jon Schuller,[2] and Ivan K. Schuller[1]

[1]*Department of Physics and Center for Advanced Nanoscience, University of California, San Diego, La Jolla, California 92093, USA*

[2]*Department of Electrical and Computer Engineering, University of California, Santa Barbara, Santa Barbara, California 93106, USA*

[3]*Material Science and Engineering Program, University of California, San Diego, La Jolla, California 92093, USA*

(Received 15 October 2018; published 5 February 2019)

The interdependences of different phase transitions in Mott materials are fundamental to the understanding of the mechanisms behind them. One of the most important relations is between the ubiquitous structural and electronic transitions. Using IR spectroscopy, optical reflectivity, and x-ray diffraction, we show that the metal-insulator transition is coupled to the structural phase transition in V_2O_3 films. This coupling persists even in films with widely varying transition temperatures and strains. Our findings are in contrast to recent experimental findings and theoretical predictions. Using V_2O_3 as a model system, we discuss the pitfalls in measurements of the electronic and structural states of Mott materials in general, calling for a critical examination of previous work in this field. Our findings also have important implications for the performance of Mott materials in next-generation neuromorphic computing technology.

DOI: 10.1103/PhysRevLett.122.057601

Despite several decades of research, the mechanism behind the metal-insulator transition (MIT) in Mott materials is still controversial [1–3]. This is partially due to concurrent changes in electronic, structural, magnetic, and orbital degrees of freedom (d.o.f.) entailed in the transition [4–6]. An example for this is the archetypical Mott material V_2O_3, which undergoes a MIT accompanied by a corundum-to-monoclinic structural phase transition (SPT) and a paramagnetic to antiferromagnetic (AFM) transition. To understand these transitions, it is imperative to determine which d.o.f. constitute the main driving force, and whether some transitions can be considered by-products of others. Fluctuations of certain d.o.f. above the critical temperature (T_C) can provide clues to identify the driving force. For instance, in the case of V_2O_3, AFM fluctuations have been reported above T_C [6,7]. More decisive evidence would be that, during the transition, some d.o.f. order before others, thereby revealing their interdependencies. It is thus of great importance to determine whether some phase transitions may decouple from others under certain circumstances. For instance, the significance of decoupling between AFM and charge ordering has been demonstrated in the perovskite rare-earth nickelates [8–14]. In VO_2, many studies have been devoted to the possibility of decoupling the MIT and SPT, with contradicting results [15–25]. Aside from the great importance of this issue for understanding the mechanisms behind the transition, decoupling between the MIT and SPT may be very useful for Mott material-based neuromorphic devices. By triggering the MIT without a concurrent SPT, the power consumption, switching time, and mechanical wear in such devices could be greatly reduced [26–29].

In V_2O_3, the relation between the structural and electronic d.o.f. in the Mott transition has been investigated recently, but a clear picture has not yet emerged. Calculations for pressure effects suggest that the SPT should precede the MIT for the paramagnetic-metal to paramagnetic-insulator transition [30]. Other calculations suggest that the corundum phase may be unstable to a monoclinic distortion even without magnetic ordering [31]. Experimentally, it was found that at very high pressure (~33 GPa) V_2O_3 stays metallic despite undergoing a monoclinic distortion [32]. In x-ray absorption fine structure measurements, indication has been found that the ~2° tilting of the c-axis vanadium pairs that occurs at the corundum-to-monoclinic transition may not be abrupt [33]. Rather, it was suggested that it starts smoothly before the full-fledged monoclinic distortion. More evidence for a structural precursor to the MIT was suggested from surface acoustic waves measurements [34] and Raman spectroscopy [35]. However, in the three latter studies, the measured precursors were compared to the resistance, which is a poor indicator for the state of the sample, as we elucidate in the present Letter (see Supplemental Material [36]). Most recently, a near-field infra-red imaging study, combined with atomic force microscopy and x-ray diffraction (XRD), analyzed the evolution of the nanoscale domain structure of V_2O_3 thin films with temperature [47]. This study found a surprising ~6 K separation between the MIT and SPT, suggesting that an intermediate monoclinic metal

may be stable close to the transition temperature. However, from pump-probe experiments a different picture emerges where an expanded-corundum insulating metastable state is photoinduced on a timescale of a few picoseconds [48]. Subsequently, metallic domains form at a rate that is limited by the speed of sound, indicating that the metallic state can form only along with the full structural transition [49,50]. These controversies have to be resolved in order to guide judicious theoretical efforts.

In this Letter, we investigated whether the SPT in V_2O_3 can decouple in equilibrium from the MIT and if decoupling can be influenced by strain. Most simply, strain couples to the structural d.o.f. by adding an elastic energy term, which may shift the free energy balance between the (low-T) monoclinic and (high-T) corundum states. Moreover, by changing the interatomic spacing, strain may also cause overlap integrals to change, leading to variations in the bandwidth and superexchange interaction, which may strongly affect the AFM ordering and MIT. In general, there is no reason for strain to affect the MIT and SPT in the same way, unless they are intimately coupled. We used temperature-dependent IR and optical reflectivity in combination with XRD to measure the electronic and structural high-temperature phase fractions across the transition. This enabled us to compare the evolution of the MIT and SPT with temperature. We applied these methods to strained films exhibiting large variations in transition temperatures. Contrary to previous work [34,35,47], we find no signature of decoupling between the structural and electronic transitions to our measurement resolution. Our findings provide a significant constraint for any theory aiming to explain the MIT in V_2O_3 and put forward important experimental considerations regarding the interpretation of similar measurements in V_2O_3, VO_2, and other Mott materials.

We grew V_2O_3 thin films on Al_2O_3 substrates of different orientations, namely, (100), (012), and (110) to obtain samples with varying T_C values. The films are 20–300 nm thick and grow epitaxially following the underlying Al_2O_3 substrate, as found in a previous study [51]. Using XRD at room temperature, we found that each orientation produces anisotropic strains of different magnitudes and in different crystallographic directions (see Supplemental Material for fabrication and structural analysis details [36–45]). This leads to deviations from perfect corundum symmetry even above the SPT temperature. The room-temperature strains in some axes are comparable in magnitude to those of the monoclinic distortion and in some cases exceed them (see Table S1). The resulting transition temperatures of the strained films span ~30 K, with lower and higher T_C values compared to bulk V_2O_3 (see Fig. 1). The thickness influences T_C somewhat, but for each thickness the order $T_C^{(110)} < T_C^{(012)} < T_C^{(100)}$ was maintained, thus corroborating the role of the substrate in determining T_C. The exact reason for this wide range of T_C variations is outside the scope of this Letter (see

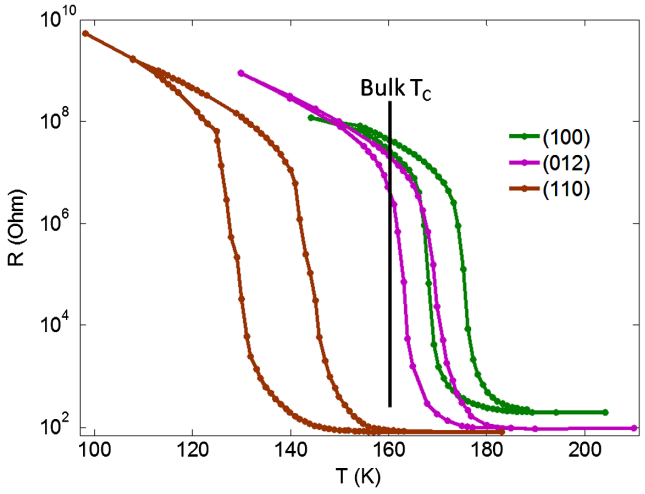

FIG. 1. Resistance vs temperature curves for three 100 nm samples of V_2O_3 grown on sapphire substrates with different orientations. A ~30 K variation in T_C is observed both above and below the T_C of bulk V_2O_3.

Supplemental Material for more details [36]). However, we can conclude that the energy scales associated with the strains are comparable to those associated with the transition, as they lead to variations of almost 20% of the bulk $T_C = 160$ K. Given these large variations in MIT temperatures, one expects that the SPT, if decoupled from the MIT, would decouple to different extents in the different films.

To study the evolution of the SPT, we used XRD to measure the temperature dependence of the out-of-plane Bragg peaks in our films. As shown in Fig. 2(a), at temperatures well above (below) the transition, a single Bragg peak is observed, indicating that the film is fully in the corundum (monoclinic) phase. At intermediate temperatures, two peaks are observed, indicating a mixture of corundum and monoclinic domains. The data were fitted with two Lorentzian+Gaussian sums that yielded an excellent approximation to the more accurate yet computationally demanding Voigt function. We note that the intensity and total area of the monoclinic peak is usually smaller than that of the corundum peak. The main reason for this is that for some monoclinic twins the diffraction conditions are not met for the out-of-plane measurement configuration, resulting in reduced intensity for the out-of-plane peak. We found that different monoclinic twins, made inequivalent due to the substrate, evolve differently in some cases with temperature. Thus, the low-temperature peak does not provide a good indication for the evolution of the total monoclinic phase fraction in the sample. However, the corundum peak is unique and as such provides an accurate account of the total corundum phase fraction (CPF), which was extracted solely from the area under the high-temperature peak fit.

Measurements of the metallic phase fraction (MPF) across the MIT were performed using Fourier transform

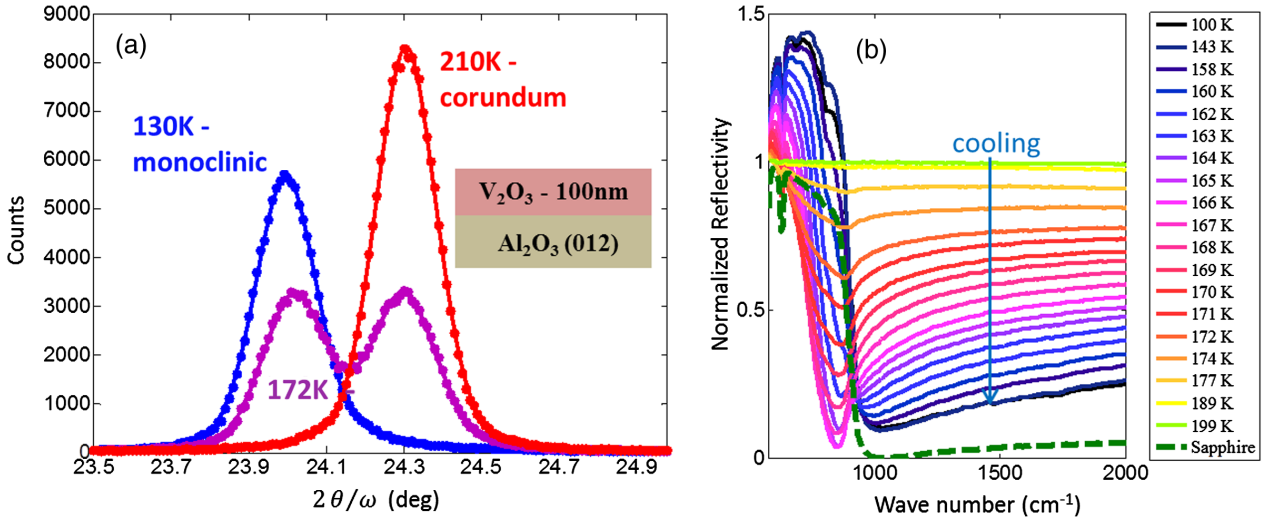

FIG. 2. Determination of high-temperature phase fractions. (a) Temperature-dependent XRD of 100 nm (012) V_2O_3 showing the evolution from the high-temperature corundum state to the low-temperature monoclinic state. Solid lines are fits to the data. The corundum phase fraction is derived from the area under the graph of the corundum peak fit. (b) Normalized FTIR spectra acquired on the same sample as in (a) while cooling. The low wave number range shows a cavity resonance centered at ~850 cm^{-1} due to the high sapphire reflectivity in this regime (green dashed curve). The V_2O_3 metallic phase fraction was extracted from the 1100–2000 cm^{-1} range. See text for more details.

IR spectroscopy (FTIR) in reflection mode (see [52] for technical details). An example of the spectra for a 100 nm V_2O_3 film as a function of temperature is shown in Fig. 2(b). The curves are normalized to the spectrum obtained at room temperature. Up to 950 cm^{-1} the spectrum is nonmonotonic with temperature showing several sharp absorptions due to phonons in the sapphire substrate, along with a broad dip at ~850 cm^{-1}, which appears only at intermediate temperatures. Very similar behavior was observed also in VO_2 films due to Fabry-Perot-like cavity resonances, which are made possible by the high reflectivity of sapphire in this regime [see green dashed curve in Fig. 2(b)] [53]. In the range 1100–2000 cm^{-1}, the sapphire reflectivity is less than 5% so that cavity resonances are strongly suppressed. In this regime, the reflectivity monotonically decreases as the sample is cooled down from the metallic to the insulating state. This is expected from the decrease in the number of free carriers due to the MIT.

To extract the MPF, we assume that the change in reflectivity is only due to the change in the metallic and insulating phase fractions and neglect the temperature dependence of the reflectivity of each pure state. The effective optical constants of the film are thus an average of the invariant optical constants of the pure metallic or insulating domains, weighted by their volume fraction [54]. This yields the following formula for the MPF as a function of temperature:

$$\mathrm{MPF}(T) = \frac{r(T) - r_I}{r_M - r_I},$$

where r_M and r_I are the reflectivity of the purely metallic and insulating states, respectively (obtained at the lowest and highest measured temperatures), and $r(T)$ is the reflectivity at temperature T. Previous work suggests that in VO_2, close to the MIT, optical constants of the pure states vary as a function of temperature even before the MIT occurs [55]. These variations were found to be strongly wave number dependent. In our case, however, we find that in the range 1100–2000 cm^{-1} the reflectivity varies negligibly at temperatures below or above the transition and the extracted MPF is almost wave number independent (see Fig. S2). Thus, significant effects of cavity resonances or intrinsic optical properties that are strongly wave number and temperature dependent can be ruled out. This supports our assumption regarding the invariance of optical constants of the pure states and reinforces the reliability of our method of extracting the MPF from $r(T)$. The extracted MPF(T) shown in Fig. 3 is an average over the range of 1100–2000 cm^{-1}.

During all temperature-dependent measurements described in this Letter, the resistance of the film was recorded and used for thermometry calibration to ensure temperature shifts between the different measurement systems were accounted for. This calibration procedure is crucial since shifts of several degrees between different systems are common. By monitoring the resistance, we have also found that the energy fluxes used in our phase fraction measurements do not perturb the state of the system. This was also confirmed by checking for reproducibility with various probe intensities (see Supplemental

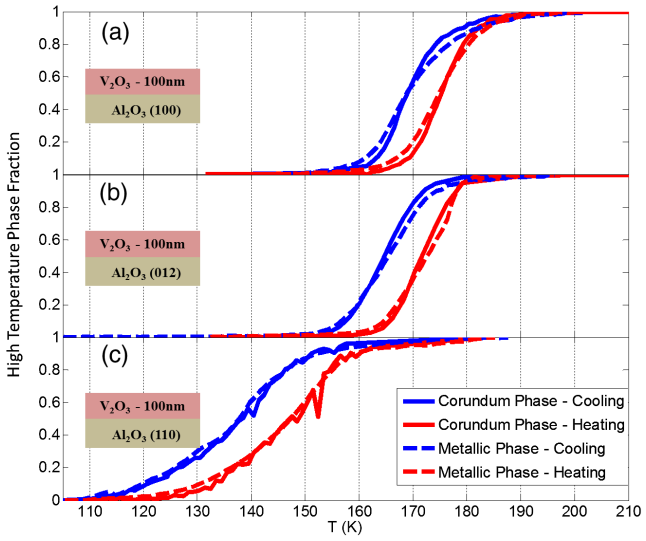

FIG. 3. Comparison between the metallic and corundum phase fractions as determined from IR spectroscopy and XRD, respectively. These measurements were performed on 100 nm films grown on sapphire substrates of different orientations. Despite large variation in transition temperatures, the electronic and structural phase transitions are coupled to our measurement accuracy.

Material for details [36]). We note that deriving the phase fraction from resistance vs temperature measurements requires exact knowledge of domain structure and is otherwise very unreliable due to the anisotropic domain configuration and percolative nature of the transition (see Supplemental Material for details [36]).

Figure 3 presents the main findings of this Letter—a comparison between the MPF(T) and CPF(T), comprising the electronic and structural high-temperature states, respectively. All measurements presented in Fig. 3 were performed on 100 nm thick V_2O_3 films grown on sapphire substrates of different orientation. Despite the large differences in the critical temperatures and strains between the three films, we found a remarkable correspondence between the MPF and CPF even though the two quantities were measured using very different techniques. This shows that the strains in our films are unable to decouple the MIT and SPT, indicating a robust coupling between them. This indicates either a causative relation between these transitions or that they share a common origin. For applications involving V_2O_3 devices, it seems that the SPT is hard to avoid and may produce a large contribution to the energy, time, and mechanical wear involved in the switching process.

In both XRD and IR measurements shown in Fig. 3, the entire thickness of the V_2O_3 films was probed. The x rays have a penetration depth of ~13 μm [56], which is 2 orders of magnitude larger than the film thickness. The penetration depth in our IR frequency range is approximately 180 and 760 nm in the metallic and insulating states, respectively. This leads to a probed depth that varies between 90 and 380 nm when measuring reflectivity. The 100 nm thick films are within the probed depth, and therefore we were able to obtain very good correspondence between the MPF and CPF.

For thicker films, however, the same procedure yielded significant differences between the apparent MPF and CPF in some cases, similar to a previous study on a film of 300 nm thickness [47]. Importantly, for the same substrate orientation, the differences in lattice parameters between 100 and 300 nm thick films (less than 0.02%) are an order of magnitude smaller than the typical strain in our films (in the range of 0.1%–1%). This shows that past a thickness of at most 100 nm the strain in our films is constant. It is thus unlikely that a decoupling of the MIT and SPT would appear in thicker films but not in thinner ones. More plausibly, we argue that the differences in the probed depth may lead to a discrepancy between the CPF and apparent MPF when the evolution of metallic or insulating domains is depth dependent. Such depth dependence was recently observed in VO_2, where domains tended to nucleate on either the top or bottom of the film and then grow to engulf the entire thickness [38].

To check if the domain evolution in our case is uniform across the thickness of the sample, we grew a 55 nm V_2O_3 film on a double-side polished sapphire substrate and measured the reflectivity from both sides of the film. For this measurement, we used a 660 nm laser that probes a depth of ~26 nm in the metallic state. More details on this measurement can be found in the Supplemental Material [36]. We note that, contrary to the IR regime, for this wavelength, the insulating state is more reflecting than the metallic state due to an increased lossiness of the metallic state and approaching a Fabry-Perot resonance in the insulating state, similar to the case of VO_2 [57]. In the laser system, we can only measure at a single wavelength,

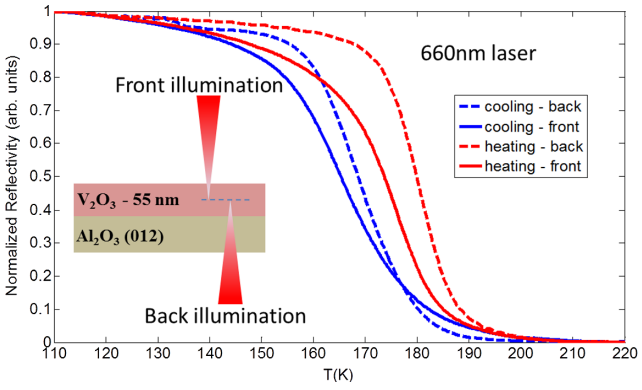

FIG. 4. Reflectivity of a 55 nm thick V_2O_3 film as a function of temperature as measured from the front (solid line) and the back (dashed line) using a 660 nm laser. The penetration depth in the metallic state is small enough to probe ~26 nm on either side of the film. Significant differences between the measurements are found, indicating that domain evolution is depth dependent even in very thin films.

making exact extraction of phase fractions unreliable, as previously discussed. Nevertheless, significant differences between the reflectivity curves as measured from the front and the back are readily observed (Fig. 4). For ease of comparison, the reflectivity curves were normalized between zero and one. The front illumination transitions are lower in temperature, significantly more smeared, and their hysteresis is smaller and closes ~10 K below their backillumination counterparts. This shows that, as in the case of VO_2, the domain evolution in our samples is depth dependent, highlighting the importance of using probes that are sensitive to the same depth. Taking into account that the nano-IR signals measured in Ref. [47] emanate from a rather shallow depth (~20 nm), it is plausible that the apparent MIT, as measured with this method, would be shifted to a lower temperature compared to the SPT, which is measured with bulk sensitive techniques in a 300 nm thick film.

In conclusion, we compared the SPT and MIT in strained V_2O_3 thin films with T_C values above and below the bulk transition temperature. Despite different strain magnitudes and orientations and ~30 K variation in transition temperature, the SPT and MIT are coupled in all films, to our measurement resolution of 1 K. This robust coupling places important constraints on the mechanism behind the MIT in V_2O_3. We note that these findings cannot preclude decoupling of phase transitions in metastable states that are not accessible in equilibrium. However, our results are consistent with findings of pump-probe experiments that suggest that, even far from equilibrium, metallic domain growth is limited by SPT timescales. Our findings also have important implications for understanding the fundamental limits on speed, reliability, and energy consumption of V_2O_3-based devices. We discuss ways to overcome common artifacts that may arise in this type of measurement in other Mott materials. Among other considerations, we show that the resistance is not a reliable way of measuring the MPF and cannot be straightforwardly compared to measurements probing other phase fractions (see Supplemental Material [36]). We also suggest a judicious way of choosing a wavelength range to accurately extract the MPF from spectroscopy measurements. Additionally, we found evidence that the temperature evolution of the domain structure is depth dependent even in very thin films, highlighting the importance of probing the same volume with different techniques for measuring the MPF and CPF. These often overlooked considerations may explain contradictions found in similar works on V_2O_3 and VO_2.

The synthesis and characterization aspects of this work were supported by the Vannevar Bush Faculty Fellowship program sponsored by the Basic Research Office of the Assistant Secretary of Defense for Research and Engineering and funded by the Office of Naval Research through Grant No. N00014-15-1-2848. The transport and optical measurements were supported through an Energy Frontier Research Center funded by the U.S. Department of Energy, Office of Science, Basic Energy Sciences under Award No. DE-SC0019273. The collaborative UCSD-UCSB research was supported by the UC Office of the President, Multicampus Research Programs and Initiatives Grant No. MR-15-328528. J. d. V. thanks the Fundación Ramón Areces for their partial support.

*Present Address: Unité Mixte de Physique, CNRS, Thales, Université Paris-Sud, Université Paris-Saclay, 91767 Palaiseau, France.

[1] M. Imada, A. Fujimori, and Y. Tokura, Rev. Mod. Phys. **70**, 1039 (1998).
[2] V. I. Anisimov, D. E. Kondakov, A. V. Kozhevnikov, I. A. Nekrasov, Z. V. Pchelkina, J. W. Allen, S.-K. Mo, H.-D. Kim, P. Metcalf, S. Suga, A. Sekiyama, G. Keller, I. Leonov, X. Ren, and D. Vollhardt, Phys. Rev. B **71**, 125119 (2005).
[3] M. J. Rozenberg, G. Kotliar, H. Kajueter, G. A. Thomas, D. H. Rapkine, J. M. Honig, and P. Metcalf, Phys. Rev. Lett. **75**, 105 (1995).
[4] D. B. McWhan and J. P. Remeika, Phys. Rev. B **2**, 3734 (1970).
[5] D. B. McWhan, J. P. Remeika, T. M. Rice, W. F. Brinkman, J. P. Maita, and A. Menth, Phys. Rev. Lett. **27**, 941 (1971).
[6] W. Bao, C. Broholm, G. Aeppli, P. Dai, J. M. Honig, and P. Metcalf, Phys. Rev. Lett. **78**, 507 (1997).
[7] J. Trastoy, A. Camjayi, J. del Valle, Y. Kalcheim, J.-P. Crocombette, J. E. Villegas, M. Rozenberg, D. Ravelosona, and I. K. Schuller, arXiv:1808.03528.
[8] S. Catalano, M. Gibert, J. Fowlie, J. Íñiguez, J.-M. Triscone, and J. Kreisel, Rep. Prog. Phys. **81**, 046501 (2018).
[9] S. B. Lee, R. Chen, and L. Balents, Phys. Rev. Lett. **106**, 016405 (2011).
[10] M. Medarde, P. Lacorre, K. Conder, F. Fauth, and A. Furrer, Phys. Rev. Lett. **80**, 2397 (1998).
[11] I. Vobornik, L. Perfetti, M. Zacchigna, M. Grioni, G. Margaritondo, J. Mesot, M. Medarde, and P. Lacorre, Phys. Rev. B **60**, R8426 (1999).
[12] J.-S. Zhou and J. B. Goodenough, Phys. Rev. B **69**, 153105 (2004).
[13] M. L. Medarde, J. Phys. Condens. Matter **9**, 1679 (1997).
[14] G. Catalan, Phase Transitions **81**, 729 (2008).
[15] S. Kumar, J. P. Strachan, A. L. D. Kilcoyne, T. Tyliszczak, M. D. Pickett, C. Santori, G. Gibson, and R. S. Williams, Appl. Phys. Lett. **108**, 073102 (2016).
[16] Y.-G. Jeong, S. Han, J. Rhie, J.-S. Kyoung, J.-W. Choi, N. Park, S. Hong, B.-J. Kim, H.-T. Kim, and D.-S. Kim, Nano Lett. **15**, 6318 (2015).
[17] Z. Tao, T.-R. T. Han, S. D. Mahanti, P. M. Duxbury, F. Yuan, C.-Y. Ruan, K. Wang, and J. Wu, Phys. Rev. Lett. **109**, 166406 (2012).
[18] B. S. Mun, K. Chen, Y. Leem, C. Dejoie, N. Tamura, M. Kunz, Z. Liu, M. E. Grass, C. Park, J. Yoon, Y. Y. Lee, and H. Ju, Phys. Status Solidi **5**, 107 (2011).
[19] M. K. Liu, M. Wagner, E. Abreu, S. Kittiwatanakul, A. McLeod, Z. Fei, M. Goldflam, S. Dai, M. M. Fogler, J. Lu, S. A. Wolf, R. D. Averitt, and D. N. Basov, Phys. Rev. Lett. **111**, 096602 (2013).

[20] B.-J. Kim, Y. W. Lee, S. Choi, J.-W. Lim, S. J. Yun, H.-T. Kim, T.-J. Shin, and H.-S. Yun, Phys. Rev. B **77**, 235401 (2008).

[21] J. Laverock, S. Kittiwatanakul, A. A. Zakharov, Y. R. Niu, B. Chen, S. A. Wolf, J. W. Lu, and K. E. Smith, Phys. Rev. Lett. **113**, 216402 (2014).

[22] M. Yang, Y. Yang, Bin Hong, L. Wang, K. Hu, Y. Dong, H. Xu, H. Huang, J. Zhao, H. Chen, L. Song, H. Ju, J. Zhu, J. Bao, X. Li, Y. Gu, T. Yang, X. Gao, Z. Luo, and C. Gao, Sci. Rep. **6**, 23119 (2016).

[23] S. Kittiwatanakul, S. A. Wolf, and J. Lu, Appl. Phys. Lett. **105**, 073112 (2014).

[24] B.-J. Kim, Y. W. Lee, B.-G. Chae, S. J. Yun, S.-Y. Oh, H.-T. Kim, and Y.-S. Lim, Appl. Phys. Lett. **90**, 023515 (2007).

[25] J. Nag, R. F. Haglund, E. A. Payzant, and K. L. More, J. Appl. Phys. **112**, 103532 (2012).

[26] Y. Zhou and S. Ramanathan, Proc. IEEE **103**, 1289 (2015).

[27] M. D. Pickett, G. Medeiros-Ribeiro, and R. S. Williams, Nat. Mater. **12**, 114 (2013).

[28] I. K. Schuller, R. Stevens, R. Pino, and M. Pechan, Neuromorphic Computing—From Materials Research to Systems Architecture (2015), https://science.energy.gov/~/media/bes/pdf/reports/2016/NCFMtSA_rpt.pdf.

[29] J. del Valle, J. G. Ramírez, M. J. Rozenberg, I. K. Schuller, J. Appl. Phys. **124**, 211101 (2018).

[30] I. Leonov, V. I. Anisimov, and D. Vollhardt, Phys. Rev. B **91**, 195115 (2015).

[31] D. Grieger and M. Fabrizio, Phys. Rev. B **92**, 075121 (2015).

[32] Y. Ding, C.-C. Chen, Q. Zeng, H.-S. Kim, M. J. Han, M. Balasubramanian, R. Gordon, F. Li, L. Bai, D. Popov, S. M. Heald, T. Gog, H. K. Mao, and M. van Veenendaal, Phys. Rev. Lett. **112**, 056401 (2014).

[33] P. Pfalzer, G. Obermeier, M. Klemm, S. Horn, and M. L. denBoer, Phys. Rev. B **73**, 144106 (2006).

[34] J. Kündel, P. Pontiller, C. Müller, G. Obermeier, Z. Liu, A. A. Nateprov, A. Hörner, A. Wixforth, S. Horn, and R. Tidecks, Appl. Phys. Lett. **102**, 101904 (2013).

[35] S. S. Majid, D. K. Shukla, F. Rahman, K. Gautam, R. J. Choudhary, V. G. Sathe, and D. M. Phase, Appl. Phys. Lett. **110**, 173101 (2017).

[36] See Supplemental Material at http://link.aps.org/supplemental/10.1103/PhysRevLett.122.057601 for growth details, structural analysis, IR and optical measurement details, and discussion of previous work on MIT and SPT decoupling in V_2O_3, which include Refs. [37–46].

[37] J. Trastoy, Y. Kalcheim, J. del Valle, I. Valmianski, and I. K. Schuller, J. Mater. Sci. **53**, 9131 (2018).

[38] D. Lee, J. Lee, K. Song, F. Xue, S.-Y. Choi, Y. Ma, J. Podkaminer, D. Liu, S.-C. Liu, B. Chung, W. Fan, S. J. Cho, W. Zhou, J. Lee, L.-Q. Chen, S. H. Oh, Z. Ma, and C.-B. Eom, Nano Lett. **17**, 5614 (2017).

[39] B. S. Allimi, S. P. Alpay, D. Goberman, T. Huang, J. I. Budnick, D. M. Pease, and A. I. Frenkel, J. Mater. Res. **22**, 2825 (2007).

[40] L. J. Eckert and R. C. Bradt, J. Appl. Phys. **44**, 3470 (1973).

[41] E. R. Dobrovinskaya, L. A. Lytvynov, and V. Pishchik, edited by V. Pishchik, L. A. Lytvynov, and E. R. Dobrovinskaya, *Sapphire: Material, Manufacturing, Applications (Micro- and Opto-Electronic Materials, Structures, and Systems)* (Springer, Boston, 2009), pp. 55–176.

[42] J. Brockman, M. G. Samant, K. P. Roche, and S. S. P. Parkin, Appl. Phys. Lett. **101**, 051606 (2012).

[43] H. Schuler, S. Klimm, G. Weissmann, C. Renner, and S. Horn, Thin Solid Films **299**, 119 (1997).

[44] Y. Ueda, K. Kosuge, and S. Kachi, J. Solid State Chem. **31**, 171 (1980).

[45] S. A. Shivashankar and J. M. Honig, Phys. Rev. B **28**, 5695 (1983).

[46] S. H. Dietze, M. J. Marsh, S. Wang, J.-G. Ramírez, Z.-H. Cai, J. R. Mohanty, I. K. Schuller, and O. G. Shpyrko, Phys. Rev. B **90**, 165109 (2014).

[47] A. S. McLeod, E. van Heumen, J. G. Ramirez, S. Wang, T. Saerbeck, S. Guenon, M. Goldflam, L. Anderegg, P. Kelly, A. Mueller, M. K. Liu, I. K. Schuller, and D. N. Basov, Nat. Phys. **13**, 80 (2016).

[48] A. Singer, J. G. Ramirez, I. Valmianski, D. Cela, N. Hua, R. Kukreja, J. Wingert, O. Kovalchuk, J. M. Glownia, M. Sikorski, M. Chollet, M. Holt, I. K. Schuller, and O. G. Shpyrko, Phys. Rev. Lett. **120**, 207601 (2018).

[49] A. Ronchi, P. Homm, M. Menghini, P. Franceschini, F. Maccherozzi, F. Banfi, G. Ferrini, F. Cilento, F. Parmigiani, S. S. Dhesi, M. Fabrizio, J.-P. Locquet, and C. Giannetti, arXiv:1807.03670.

[50] E. Abreu, S. Wang, J. G. Ramírez, M. Liu, J. Zhang, K. Geng, I. K. Schuller, and R. D. Averitt, Phys. Rev. B **92**, 085130 (2015).

[51] I. Valmianski, J. G. Ramirez, C. Urban, X. Batlle, and I. K. Schuller, Phys. Rev. B **95**, 155132 (2017).

[52] N. A. Butakov and J. A. Schuller, Sci. Rep. **6**, 38487 (2016).

[53] M. A. Kats, D. Sharma, J. Lin, P. Genevet, R. Blanchard, Z. Yang, M. M. Qazilbash, D. N. Basov, S. Ramanathan, and F. Capasso, Appl. Phys. Lett. **101**, 221101 (2012).

[54] G. L. Carr, S. Perkowitz, and D. B. Tanner, *Infrared and Millimeter Waves* (Academic Press, Inc., Orlando, 1985).

[55] M. M. Qazilbash, M. Brehm, B.-G. Chae, P.-C. Ho, G. O. Andreev, B.-J. Kim, S. J. Yun, A. V. Balatsky, M. B. Maple, F. Keilmann, H.-T. Kim, and D. N. Basov, Science **318**, 1750 (2007).

[56] B. L. Henke, E. M. Gullikson, and J. C. Davis, At. Data Nucl. Data Tables **54**, 181 (1993).

[57] N. A. Butakov, I. Valmianski, T. Lewi, C. Urban, Z. Ren, A. A. Mikhailovsky, S. D. Wilson, I. K. Schuller, and J. A. Schuller, ACS Photonics **5**, 371 (2018).